Desalination 518 (2021) 115267

Contents lists available at ScienceDirect

Desalination

journal homepage: www.elsevier.com/locate/desal

Simultaneous energy production, boron and COD removal using a novel microbial desalination cell

A.Y. Goren [a], H.E. Okten [a,b,*]

[a] Izmir Institute of Technology, Department of Environmental Engineering, İzmir, Turkey
[b] Environmental Development Application and Research Center, İzmir, Turkey

HIGHLIGHTS

- A novel MDC design with 3D cubic electrodes was developed.
- Activated sludge to wastewater volumetric ratio was studied for the first time.
- Results with 3D and 2D electrodes were comparable.
- Novel 3D design is promising for scaled-up applications.

GRAPHICAL ABSTRACT

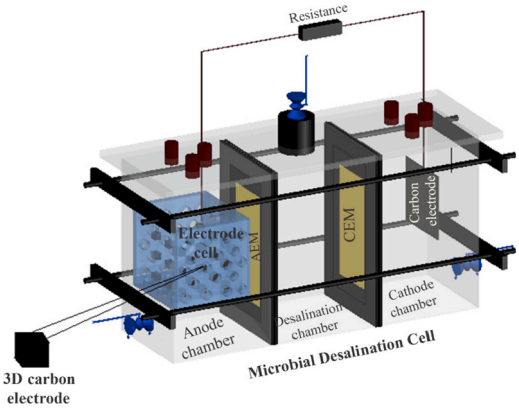

ARTICLE INFO

Keywords:
Microbial desalination cell
3D cubic electrodes
Boron removal
Energy production
Geothermal water

ABSTRACT

This paper investigates simultaneous boron removal from aqueous solutions, organic matter removal from industrial wastewater and energy production using a Microbial Desalination Cell (MDC). Anode chamber of the conventional MDC cell was modified to include 3D cubic electrodes as a novel design. Effects of operating parameters, including electrode type (3D-electrode and 2D-electrode), anolyte solution temperature (20 °C, 40 °C, and 60 °C), and activated sludge:wastewater volumetric ratio (S:WW = 1:1, 1:2, and 1:5), on MDC performance were studied. Furthermore, real geothermal water treatment was investigated under optimum operating conditions. Boron and organic matter removal efficiencies and the produced power density results were promising for 3D-electrodes under optimum operating conditions. The maximum boron removal efficiency, COD removal efficiency, and power density were 55.5%, 91.5%, and 9.04 mW/m^3 treating real geothermal water at optimum operating conditions. The analyses of Scanning Electron Microscope with Energy Dispersive X-ray spectrometer (SEM-EDX) demonstrated biofilm formation and salt deposition on membrane surfaces, which most probably reduced the performance of MDC. Consequently, our results showed that use of 3D-electrodes was a promising

* Corresponding author at: Izmir Institute of Technology, Department of Environmental Engineering, İzmir, Turkey.
E-mail address: haticeokten@iyte.edu.tr (H.E. Okten).

https://doi.org/10.1016/j.desal.2021.115267
Received 7 June 2021; Received in revised form 10 July 2021; Accepted 24 July 2021
Available online 5 August 2021

improvement to the conventional configurations with 2-D electrodes since removal efficiencies and energy production were comparable for a more compact electrode structure.

1. Introduction

In the era of climate change, water scarcity drives the inevitable paradigm shift regarding water resources and as a result, unconventional water resources are also being used to compensate for the decrease in the quantity of conventional ones. Geothermal water emerges as an important alternative water source to supply the demand for drinking, domestic, agricultural and industrial purposes. However, geothermal water sources may contain components of unfavorable nature or of unacceptable levels due to hydrogeology of aquifers and anthropogenic sources, hindering the exploitation of geothermal water resources [1,2]. Geothermal waters can be characterized by diverse physicochemical parameters depending on their hydrogeological properties, characteristics of the rocks involved, the depth at which resources occur and the source of water supply. Geothermal waters may contain significant amounts of neutral species, cations and anions [3,4]. These parameters largely determine the technology to be used in geothermal water treatment in regard with the relevant limits that are dictated by the final use. Amongst the ions that are present, boron content is critical in geothermal waters, which contain higher concentrations than sea water and brackish water.

Boron in geothermal waters has been found due to natural sources including soils containing borosilicate and borate, mineral dissolution from rocks, and volcanic activities or anthropogenic sources like cleaning products, detergents, borosilicate glass, semiconductors, fertilizers, and flame retardants production [5]. Boron species in geothermal waters and boron rich thermal springs are commonly found as undissociated boric acid (H_3BO_3) and tetrahydroxoborate ions ($B(OH)_4^-$) [6]. At low pH values in geothermal water sources, H_3BO_3 is the dominant species (the uncharged form of boron), while above pH 9.2, negatively charged $B(OH)_4^-$ is the dominant species [7,8].

Long term exposure to boron through drinking water and/or vegetables may cause several symptoms such as diarrhea, dermatitis, nausea, lethargy, and also more severe issues such as physical and intellectual setbacks at children, nonfunctional cardiovascular, nervous, and reproductive systems [9–12]. The limit values recommended for boron in drinking water from WHO and European Union (EU) are 2.4 mg/L and 1 mg/L, respectively [13,14]. In Turkey, the maximum permissible level of boron in drinking water is set at 1 mg/L by Directive of Water Intended for Human Consumption [15]. Furthermore, boron is an important micronutrient for plants, its required levels for growth depend on the plant type. Reported tolerable boron concentrations in irrigation water for plant growth vary, for instance as asparagus, palm, bean, and onion may be able to tolerate 4 mg/L B, blackberry and lemon orchards may tolerate only 0.5 mg/L B. [6,16]. Exposure to boron above tolerance levels may be detrimental for plants [17]. Therefore, in the case of using geothermal brine as irrigation water, removal of boron becomes a critical and challenging topic.

Several techniques have been developed for treatment of boron in water and wastewater, including coagulation, sedimentation, filtration, adsorption, membrane processes such as reverse osmosis (RO), biological process, ion-exchange, electrocoagulation, electrodialysis, and hybrid processes [18–22]. However, most of these technologies have numerous disadvantages such as high operating and maintenance costs, high amount of sludge formation and chemical consumption, need for additional pretreatment, and high energy consumption. Bioelectrochemical systems (BESs) are promising, emerging, and environmentally friendly technologies compared to conventional treatment processes [23,24]. The most studied BESs are microbial fuel cells (MFCs) and microbial desalination cells (MDCs), which convert chemical energy from organic matter to electrical energy using microorganisms [25–27]. While MFCs and MDCs are able to couple biological wastewater treatment with energy production, MDCs are also able to perform desalination. Microbial desalination cell (MDC) is practically derived from MFCs by inserting (i) an anion exchange membrane (AEM) between anode chamber and desalination chamber and (ii) a cation exchange membrane (CEM) between desalination and cathode chambers [25]. Electrons that are produced due to oxidation of organic substrates at anode chamber, which is kept strictly anaerobic, are given to the circuit connecting anode and cathode electrodes. The objective is to form an electrochemical gradient across the oxidative anodic and reductive cathodic chambers, facilitating the desalination process. Migration of ions in desalination cell across the membranes based on concentration and electrochemical gradients through diffusion is the driving force for desalination process.

However, MDCs present several drawbacks such as low removal efficiency, membrane fouling, low energy production due to the electrode type and material, and decrease in microbial activity related to salinity increase [28,29]. Moreover, the commonly used carbon felt, carbon paper, and graphite felt electrode materials in MDC have significant drawbacks, such as low electrode surface area for microbial colonization and organic substrate transport, unsuitable surface to form biofilm layer by microorganisms, difficulties of maintenance, and low flexibility [24,30,31]. Recently, research on investigation of three dimensional (3D) carbonaceous electrodes have attracted interest owing to their significant benefits on BES performance such as, high surface area and easy multiple direction transport of pathways with macro-porous structure, and high electron storage capacity [32–34]. The MFCs were enhanced with modifying the electrodes with 3D nano-sized and porous materials including, N-doped carbon cloth, biochar, carbon nanotube-chitosan modified carbon paper, graphene/polyaniline nanocomplex modified carbon cloth, and graphene/polyaniline modified carbon paper [35–37]. However, there is only one research article investigating the potential of MDC with 3D sponge electrode coated using carbon nanotube-chitosan [24]. The MDC using 3D sponge electrode showed a high power density of 1776.6 mW/m^2 and desalination rate of 16.5 mg/h, which were considerably higher than those of two dimensional (2D) carbon felt electrodes under same operating conditions. It should be noted that these materials were also prone to some drawbacks such as, high cost, difficult synthesis, and requirement of advanced facilities [34,38]. Therefore, studies related to electrode material and type have attained significant attention. Moreover, several studies investigated the performance of MDCs on wastewater treatment, desalination, and energy production under different operating conditions [39–41]. Catholyte solution, anolyte solution, temperature, initial salt concentration, intermembrane distance, retention time, and mode of operation were widely investigated operating parameters for optimization of MDC process [42–45]. Ebrahimi et al. [46] investigated the performance of MDC for energy production and salt removal using different catholythes such as phosphate buffer solution (PBS), non-buffer saline solution, and bio-catholyte. The MDC using bio-catholyte solution showed the highest power density (32.6 W/m^3) and desalination rate (0.38 g NaCl/Lh), while the power density and desalination rate of MDC with saline buffer solution were 29.4 W/m^3 and 0.34 g NaCl/Lh, respectively. Effects of retention time (30–120 min), temperature (mesophilic, thermophilic, and psychrophilic), and dissolved oxygen concentration (2–6 mg/L) on MDC process for optimization of arsenic removal from aqueous solution were investigated in a separate study [47]. The maximum arsenic

removal efficiency of 56% was achieved at temperature range of 25–30 °C, retention time of 120 min, and dissolved oxygen concentration of 6 mg/L.

In this study, we designed a novel MDC reactor with 3D cubic electrodes contained in a cell, which was placed in the anode chamber. We investigated and compared the performance of MDC with 2D and 3D cubic electrodes in removing boron from synthetic solutions and real geothermal water and in removing COD from yeast industry wastewater, all the while producing energy. Objectives of this study were investigating (i) the effects of activated sludge volume, anolyte temperature, and electrode type on 3D-MDC performance in batch mode operation, (ii) effect of operational parameters on energy production of 3D-MDC, and (iii) performance of the optimized system in removal of boron from real geothermal water using 3D cubic electrodes and 2D carbon graphite electrode. It should be noted that this is the first study investigating the effect of activated sludge volume and presenting performance of MDC on boron removal from real geothermal water. Consequently, this study is the first and most comprehensive research paper on applicability of conventional 2D-MDC and novel 3D-MDC for simultaneous boron removal, wastewater treatment, and energy production at optimum operating conditions.

2. Materials and methods

2.1. Characterization and preparation of water samples

Geothermal water was collected from geothermal power plant deep wells located in İzmir, Turkey and was kept in polyethylene containers throughout experiments. All species present in geothermal water were analyzed using American Public Health Association (APHA) standard methods [48]. Characterization of geothermal water yielded the following results, EC: 1770 μS/cm, pH: 8.04, K: 30.1 mg/L, Na: 452 mg/L, Ca: 24.8 mg/L, Mg: 7.44 mg/L, SO_4^{2-}: 178 mg/L, Mn: 0.027 mg/L, Cl^-: 205 mg/L, F^-: 8.21 mg/L, SiO_4^{4-}: 24 mg/L, As: 0.17 mg/L, B: 10.48 mg/L, Fe: 0.055 mg/L, and Li: 1.41 mg/L. Industrial wastewater was collected from a yeast production facility's wastewater treatment plant in İzmir. Industrial wastewater was also characterized, pH: 7.72, COD: 9228 mg/L, K: 868 mg/L, NH_4^+: 452 mg/L, NO_3^-: 25.6 mg/L, Na: 1608 mg/L, Ca: 299 mg/L, Mg: 77.5 mg/L, SO_4^{2-}: 1117 mg/L, PO_4^{3-}: 7.68 mg/L, Mn: 0.183 mg/L, Cl^-: 1573 mg/L, F^-: 0.2 mg/L, SiO_4^{4-}: 66 mg/L, As: 0.007 mg/L, B: 0.142 mg/L, and Fe: 0.571 mg/L. Synthetic boron (B) solutions were prepared daily by dissolving boric acid salt (H3BO3, Sigma-Aldrich). Solution B concentrations simulated geothermal water composition of Turkey [49,50]. Solution pH was adjusted to pH 9.5 using 0.1 M sodium hydroxide (NaOH, Sigma-Aldrich). Catholyte solution was prepared using 10 mM potassium phosphate buffer (K-PB).

2.2. MDC set up and operation

MDC bioreactor consisted three identical plexiglass chambers: anode, desalination, and cathode chambers, with dimensions of 15 cm × 6 cm × 6 cm (Fig. 1a). Chambers were clamped together using gaskets and O-rings with stainless steel bolts in order to prevent leakage. Anode and desalination chambers were separated by an anion exchange membrane (AEM, AMI-7001, Membrane International Inc., USA) while cathode and desalination chambers were separated by a cation exchange membrane (CEM, CMI-7000, Membrane International Inc., USA). Carbon graphite material was used for 2D electrodes (GoodFellow, England). Our previous studies have shown 36 cm^2 to be the optimum electrode area for 2D electrodes in our MDC system [51]. The novel MDC design accommodated a plexiglass electrode cell in the anode chamber, with dimensions of 6 cm × 4.5 cm × 4.5 cm, bearing 9 mm^2 holes on its surfaces (Fig. 1b). The electrode cell held 1 cm^3 3D cubic electrodes (Walfront, Canada) each having a surface area of 6 cm^2. In both cases, 2D and 3D electrodes, electrical connection between electrodes was done via copper wiring.

Anode chamber was filled with anaerobic activated sludge and yeast wastewater mixtures of varying volumetric ratios (S:WW = 1:1, 1:2, and 1:5) and the mixtures were continuously stirred (185 rpm) to prevent settling. Cathode chamber was filled with phosphate buffer and it was aerated at a rate of 2 L/min with air. Desalination chamber was filled with boron containing solutions or geothermal wastewater. The initial boron concentration was selected as 5 mg/L as an optimum concentration for MDC with 2D electrodes based on our previous study [51]. Anolyte solution temperatures (20 °C, 40 °C, and 60 °C) and electrode geometry at optimum conditions were investigated. Based on the preliminary studies, the reactor was operated for 12 days, the day marking 90% substrate degradation based on COD measurements. During experiments, voltage values were recorded to calculate the power density of the system.

2.3. Analytical methods

Voltage (V) in the open circuit of MDC was recorded every 15 min using a data logging system (UNI-T, UT71C Digital Multimeter). Daily pH changes were measured by a pH meter and adjustments were done (Mettler Toledo, SevenCompact™). Samples from experimental runs were collected daily, acidified using 0.1 N HCl, and then stored at 4 °C

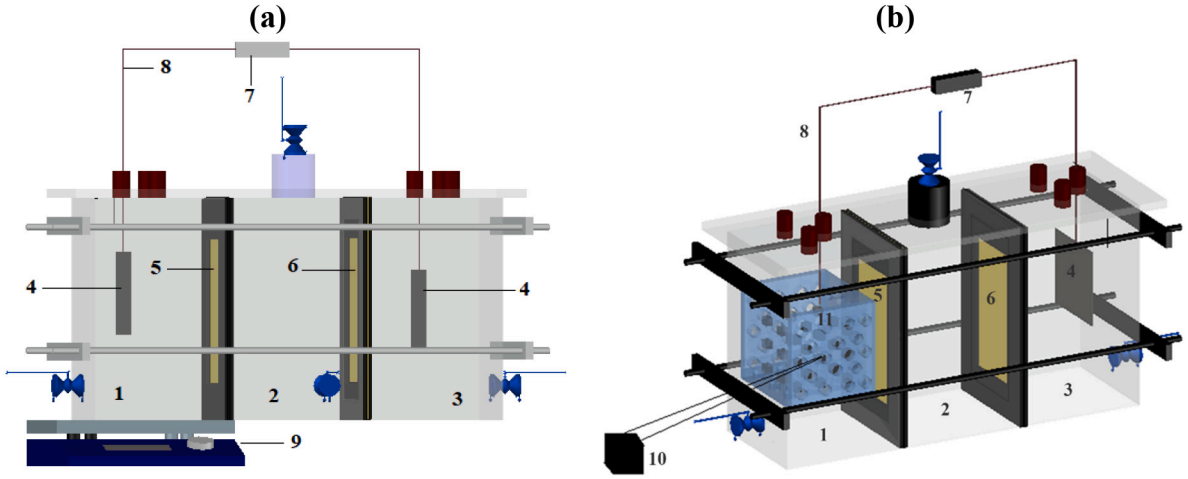

Fig. 1. The schematic diagram of MDC bioreactor: (1) Anode chamber, (2) Desalination chamber, (3) Cathode chamber, (4) Carbon graphite electrode, (5) AEM, (6) CEM, (7) External resistor, (8) Copper wire, (9) Mechanic stirrer, (10) 3D cubic electrode, and (11) anode electrode cell.

until analysis. Boron concentrations were measured using an inductively coupled plasma optical emission spectrometer (ICP-OES, AGILENT 5110). Anions and cations in water samples were measured using ion chromatography (IC, Dionex ICS-5000). All analyses were conducted in triplicate measurements. COD was measured using a closed reflux titrimetric method according to standard methods [52]. AEM and CEM surface morphologies were examined by scanning electron microscopy (SEM, Quanta-250FEG). Furthermore, elemental mapping of membrane surfaces was done using Energy dispersive X-ray spectrometry (EDX, Quanta-250FEG).

Boron and COD removal efficiencies were calculated following the Eqs. (1) and (2), respectively:

$$R_B(\%) = \left(C_{B,i} - C_{B,e}\right)/C_{B,i}*100 \quad (1)$$

$$R_{COD}(\%) = \left(C_{COD,i} - C_{COD,e}\right)/C_{COD,i}*100 \quad (2)$$

$C_{B,i}$ and $C_{B,e}$ were the initial and effluent boron concentrations in desalination chamber, respectively. $C_{COD,i}$ and $C_{COD,e}$ were the initial and effluent COD concentrations in anode chamber, respectively.

Current (I) under 100 Ω external resistance (Rex) was determined by $V = I \times R_{ex}$. Power density (P, mW/m^3) was determined through $P = V \times I/v$, where v (m^3) was the volume of the anode chamber. Furthermore, the ratio of transferred electric charge (1) to its maximum value obtainable (coulombic efficiency - CE, %), and (2) to total e^- available in the anode chamber (coulombic recovery - CR, %) were calculated by Eqs. (3) and (4), respectively:

$$CE(\%) = \frac{MW_{O2}\int_0^t Idt}{nFV_a\left(C_{COD,i} - C_{COD,e}\right)}*100 \quad (3)$$

$$CR(\%) = \frac{MW_{O2}\int_0^t Idt}{nFV_a\left(C_{COD,i}\right)}*100 \quad (4)$$

MW_{O2} was the molecular weight of oxygen (32 g/mol), n was number of the e^- transferred from organic matter degradation (n: 4 mol e^-/mol), F was the Faraday's constant (96,485 C/mol), and V_a was the volume of anode chamber (0.54 L).

3. Results and discussion

3.1. Effect of activated sludge volume

The major energy production mechanism of bioelectrochemical systems depended on the biodegradation of organic matter from various types of sludge or wastewater by microbial activity [45,53]. Microbial growth in the absence of an electron acceptor was one of the main factors that determined the performance of MDCs. Hence,

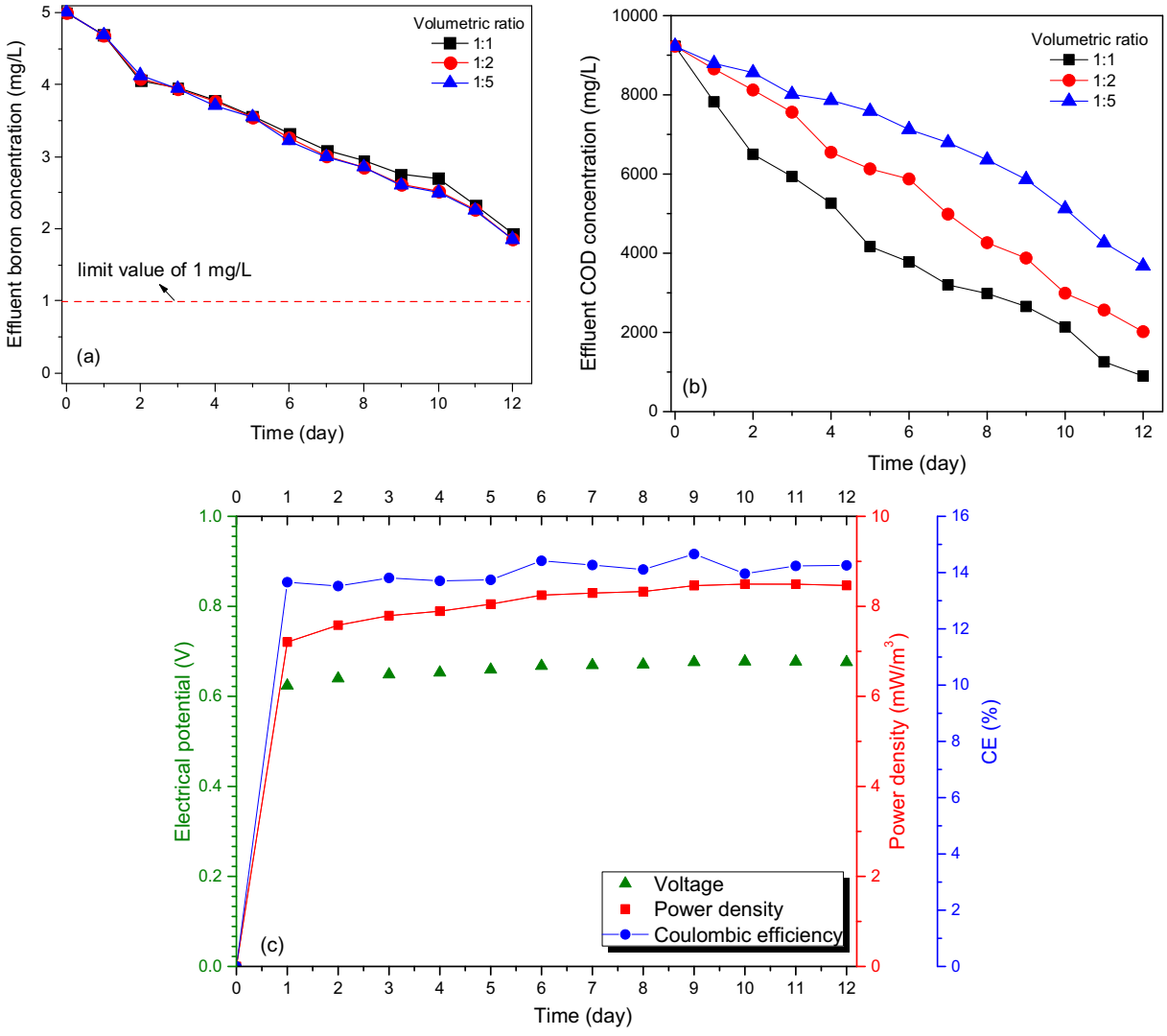

Fig. 2. Effect of varying volumetric ratios on boron removal (a) and COD removal (b); electrical potential, power density, and Coulombic efficiency at optimum volumetric ratio of 1:1 (c).

understanding microbial growth mechanisms, medium composition, organic matter concentration, the activated sludge or wastewater types and microorganism physiology would help to improve the MDC efficiency [44,54–60]. Anaerobic activated sludge volume's effect on MDC performance has not been studied before.

In this study, we varied the S:WW parameter (1:1, 1:2, and 1:5) and investigated its effect on B removal (Fig. 2a) and COD removal (Fig. 2b). While varying S:WW did not have a significant effect on B removal efficiency (62%), increasing activated sludge's volume from 90 mL (1:5) to 270 mL (1:1) improved COD removal efficiency from 60.1% to 90.3%. Charge-selective diffusion of ionic species through the membrane is the main driving mechanism in desalination with MDC. That mechanism can be further enhanced by concentration and electrochemical gradients. Since the boron concentration used in this part of the study was low (5 mg/L), the concentration gradient's improving effect on the rate of diffusion was not present. Although increasing S:WW values were expected to form an electrochemical gradient, which in turn would enhance the diffusion rate and thus removal efficiency, it was not possible to discern the data points for each experimental run due to the low initial concentration of boron. In order to elucidate the effect of concentration gradient, the removal rate of 0.256 mg B/Ld, which was acquired for S:WW of 1:1, was compared with results from Goren and Okten [51] for 10 mg/L and 20 mg/L initial boron concentrations. Results showed considerable improvements in removal rate, 0.343 mg B/Ld for 10 mg B/L and 0.7 mg B/Ld for 20 mg B/L.

The considerably low COD removal efficiencies at S:WW of 1:5 and 1:2 were probably due to the low microbial concentration and hence activity in anolyte. These results also showed that decreased activated sludge volumes implied longer operating periods in order to meet required COD removal efficiencies. Throughout the study, calculated standard deviation values for the replicates were too low (below 0.1 mg/L) to be discerned on the plots.

The open circuit voltage (OCV) of the system was recorded to be 452, 646, and 676 mV for S:WW of 1:5, 1:2, and 1:1, respectively (Fig. S1a). The power density of the system increased from 3.78 to 8.46 mW/m^3 with the increase in volumetric ratio from 1:5 to 1:1 (Fig. S1b). The higher OCV and power density produced at higher activated sludge volumes were likely due to higher energy production with increasing microbial activity (Fig. 2c). Similarly, the CE and CR values of the system increased with the increasing S:WW. The maximum CE values were 14.26%, 13% and 12.9% for ratios of 1:1, 1:2, and 1:5, respectively. Also the CR values followed a decreasing trend of 11.66%, 11.14%, and 7.79% for decreasing activated sludge volumes of 270 mL, 180 mL and 90 mL, respectively. As can be seen in Eqs. (3) and (4), the CE and CR

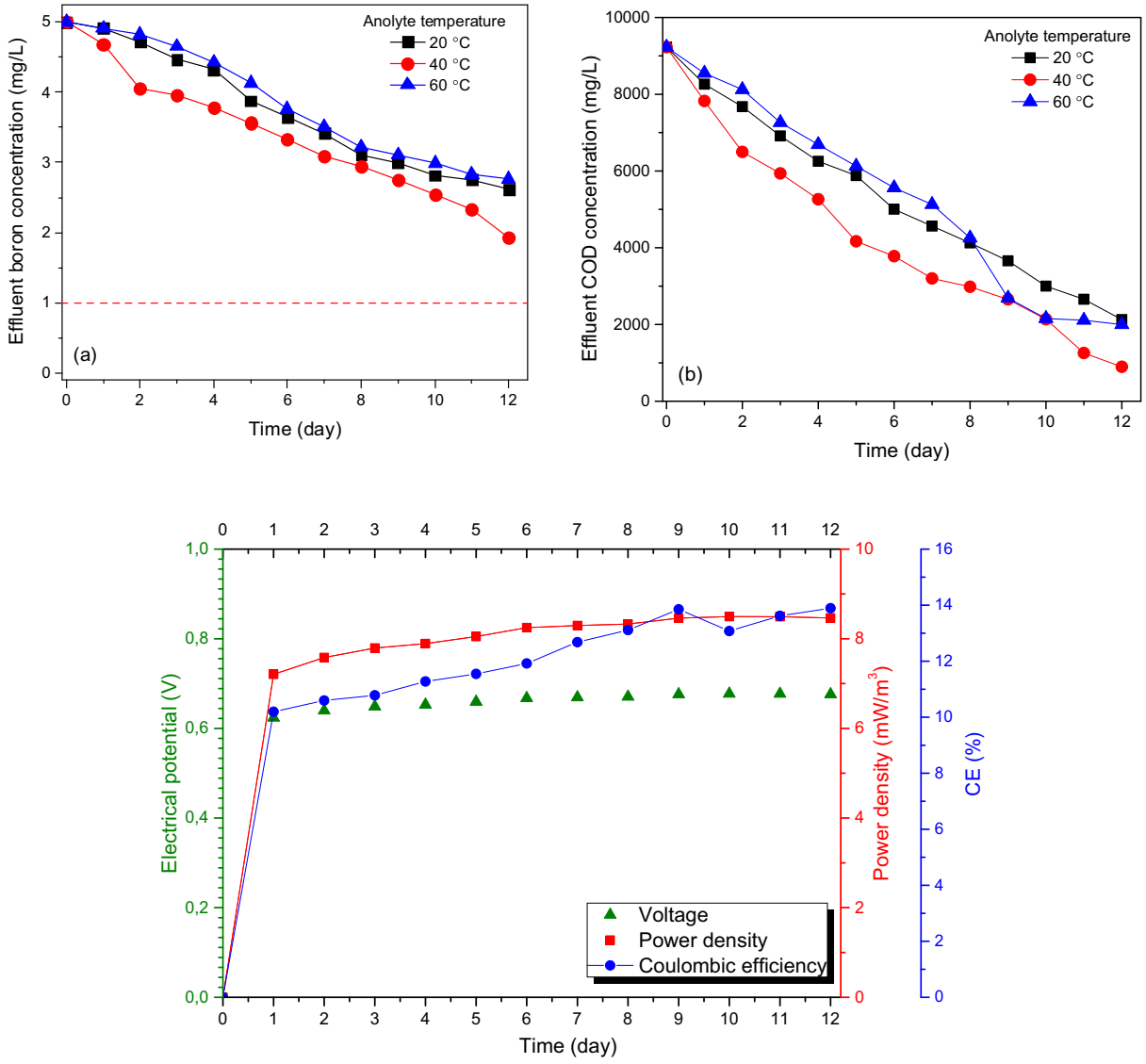

Fig. 3. Effect of anolyte temperature on boron removal (a), COD removal (b), electrical potential (c), and power density (d).

values were expected to decrease with increase in the initial COD concentration in anode chamber. Therefore, the simultaneous increase in OCV, power density, CE, and CR being observed at 1:1 ratio was due to increasing COD removal efficiency in anode chamber with the increasing microbial activity for organic matter degradation. Our results were also in good agreement with the literature. For instance, in an MFC study CE values of 10% and 25% were reported when the organic loading was increased from 500 mg/L to 4500 mg/L, respectively [61].

3.2. Effect of anolyte solution temperature

Temperature is another important operating parameter that may significantly impact the performance of bioelectrochemical systems. Factors such as internal resistance, solution conductivity, electrode potential, and microbial growth that may affect the MDC performance are all temperature dependent [62,63]. Low operating temperatures, i.e. room temperature, at MDC system can be cost effective, which reduce the requirement for external power for heating. Although MFC performances under different temperatures have been investigated before [64–66], there are limited studies for MDCs [47,67,68].

In this study, three different anolyte solution temperatures (20 °C, 40 °C, and 60 °C) were investigated for previously determined optimum operating conditions ($pH_{catholyte}$: 6.5, Q_{air}: 2 L/min, V_{sludge}: 270 mL, $V_{wastewater}$: 270 mL, C_{Boron}: 5 mg/L, $S_{electrode}$: 36 cm^2). As presented in Fig. 3a, the highest boron removal efficiency of 61.3% ($C_{f,B}$: 1.93 mg/L) was observed at anolyte temperature of 40 °C. Boron removal efficiencies were also found to be 47.7% ($C_{f,B}$: 2.62 mg/L) and 44.7% ($C_{f,B}$: 2.76 mg/L) for anolyte temperature of 20 and 60 °C, respectively. Anaerobic processes are commonly maintained at 30 °C - 40 °C (mesophilic) and 50 °C - 60 °C (thermophilic) temperature ranges [69]. At mesophilic temperatures, the metabolic rate of microorganisms increases resulting in better substrate degradation rates [70,71], accelerated electron generation by microorganisms, increasing current production and hence improving desalination efficiency [72]. Therefore, the mesophilic anolyte solution temperature of 40 °C yielded the best B removal efficiency. On the other hand, temperatures of 20 °C and 60 °C resulted in similar removal efficiencies. The metabolic activity of microorganisms decreases at temperatures below 20 °C (psychrophilic). In thermophilic temperatures, the microbial growth and decay are faster with enhanced metabolic activity, which reduces the removal of ions [47]. Mirzaienia et al. [73] investigated the nickel and lead removal from industrial wastewater using MDC and reported that the highest removal efficiency was achieved at mesophilic temperature. In another study of Malakootian et al. [47] the maximum arsenic removal efficiency was 68% at optimum operating conditions (dissolved oxygen concentration of 6 mg/L, mesophilic temperature, operating time of 120 min) for the studied MDC setup.

COD removal efficiencies were 76.9% ($C_{f,COD}$: 2128 mg/L), 90.3% ($C_{f,COD}$: 897 mg/L), and 78.3% ($C_{f,COD}$: 1998 mg/L) for anolyte temperatures of 20 °C, 40 °C, and 60 °C, respectively (Fig. 3b). As expected, the highest removal efficiency was obtained at 40 °C owing to faster substrate degradation. Expectedly, the COD removal efficiency decreased significantly at 20 °C with the decrease in microbial activity rate. Furthermore, the effluent COD concentration remained constant at 60 °C after the 10th day most probably due to faster growth and decay rates of microorganisms.

The results on OCV and power density showed that the energy production performance of the system was also affected by anolyte solution temperature (Fig. 3c). We observed that at the operating time of 12 days, OCV was 676 mV at anolyte solution temperature of 60 °C, which was almost 1.2 times higher than 20 °C (571 mV) and 60 °C (556 mV) results (Fig. S2a). The highest power density values were found to be 6.04 mW/m^3, 8.46 mW/m^3, and 5.73 mW/m^3 for anolyte solution temperatures of 20 °C, 40 °C, and 60 °C, respectively (Fig. S2b). These results most probably explained with that the microbial activity rates for microorganism growth and organic matter degradation were increased with increasing temperature up to a certain temperature that microorganisms can live [74]. Besides, increasing microbial growth may also enhance biofilm formation at an electrode surface. The conductivity of the anolyte solution is increased with increase in temperature as reported Arhenius Laws and thus the electron transfers increases [75]. Furthermore, according to the Bulter-Volmer equation [76], the reactions on the electrode surfaces are increases at high temperatures. On the other hand, as mentioned before, in thermophilic temperatures (>60 °C), the energy production efficiency of the system decreases due to the faster decay of microorganisms.

Similar trends were observed for the CE and CR values of the MDC system. The CE and CR values were 12.9% and 9.9%, 13.9% and 11.7%, and 12.8% and 9.6% for temperatures of 20 °C, 40 °C, and 60 °C, respectively. As expected, the highest CE and CR values were obtained at 40 °C. Consequently, our results suggested that the MDC at moderate anolyte solution temperature (40 °C) was possible for real application for geothermal brine treatment with higher energy production.

3.3. Effect of electrode type

The electrode material affects the MDC's performance in terms of desalination efficiency, energy production, and wastewater treatment. Recently, researchers focused on the development of three-dimensional electrode materials due to their high effective surface area which is favorable for biofilm growth, and high conductivity which can provide efficient electron transfer between the microorganisms, high charge storage capability and electrolyte penetration [77,78]. Therefore, we designed a novel MDC system with 3D cubic carbon electrodes to improve the effective use of electrode materials.

The effect of novel electrode cell with 3D cubic carbon electrodes on boron and COD removal efficiencies was compared with the carbon plate electrode material (Fig. 4a and b). The electrode surface areas of both electrodes was selected as 36 cm^2 (V_{sludge}: 270 mL, Q_{air}: 2 L/min, $V_{wastewater}$: 270 mL, $pH_{catholyte}$: 6.5, $T_{anolyte}$: 40 °C, and operating time: 12 days). The boron and COD removal efficiencies increased with 3D cubic electrodes. Boron removal efficiencies were measured as 61.3% ($C_{f,B}$: 1.934 mg/L) and 64.9% ($C_{f,B}$: 1.756 mg/L) for 2D and 3D electrodes, respectively. The increase in boron removal efficiency with 3D cubic electrodes was most probably due to the increasing ion transfer with the increase in microbial activity owing to enhanced available electrode surfaces for microbial growth. Furthermore, when plate electrodes were used in the anode cell, it was not possible to operate the system using high electrode surface areas due to the anode chamber size, but thanks to the novel electrode cell, it was possible to work in higher surface areas taking up less space. The COD removal efficiencies using plate and 3D cubic electrodes were quite similar. The highest COD removal efficiencies were 90.3% ($C_{f,COD}$: 897 mg/L), and 90.7% ($C_{f,COD}$: 856 mg/L) for 2D and 3D electrodes, respectively.

There are limited number of studies on boron removal using MDC from synthetic solutions and real water resources [26,51]. Ping et al. [26] studied boron removal from synthetic solutions using MDC process with Donnan dialysis pretreatment system and they reported that the highest boron removal efficiencies were found to be 60 and 52% at initial boron concentration of 5 and 20 mg/L, respectively. In our previous study, the highest boron removal efficiency using MDC was found to be 45.2% under optimized conditions (electrode surface area of 36 cm^2, catholyte solution of phosphate buffer, operating time of 12 days, initial boron concentration of 5 mg/L, and air flow rate of 2 L/min), while the highest removal efficiency was 39.4% for initial boron concentration of 10 mg/L at same operating conditions [51]. Moreover, the maximum boron removal from real geothermal water was found as 44.3% at optimized conditions.

The MDC energy production performance was investigated with respect to two different electrode type under optimum operating conditions (Fig. 4c). On the tenth day, MDC achieved the maximum voltage of almost 680 mV for 2D plate type electrode (Fig. S3a). Voltage was

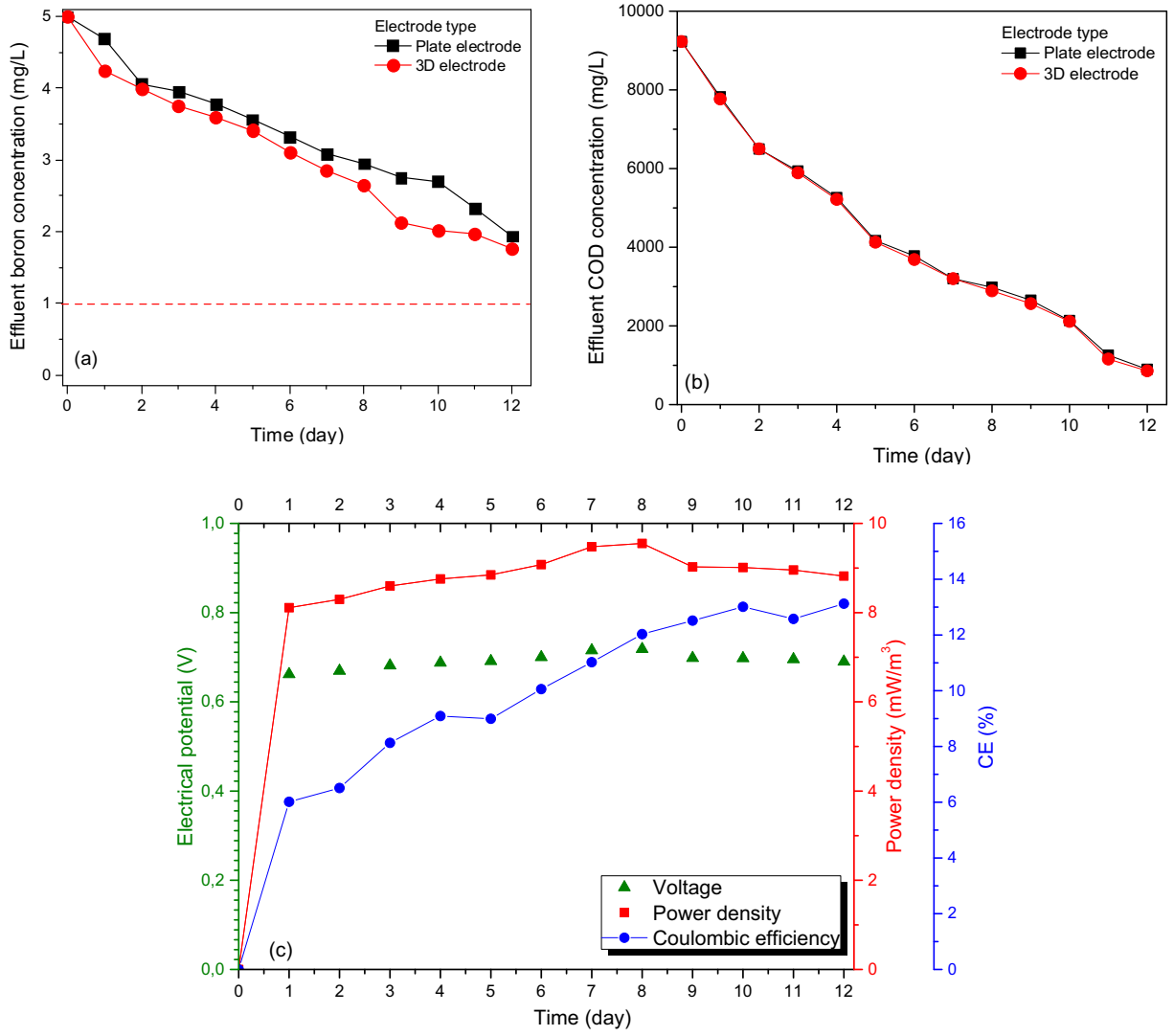

Fig. 4. Effect of electrode type on boron and COD removal efficiency.

almost stable at maximum voltage for 2 days which indicated steady microbial growth, producing electrons for the energy production at the anode chamber. Furthermore, to understand the power density, anode and cathode chambers were connected with an external resistance of 100 Ω. Results showed that the power density increased with time and attained the maximum power density of 8.50 mW/m^3 in 10 days for 2D plate electrode (Fig. S3b). After that, the power density decreased with operating time which might be attributed to the depletion of organic matter at the anode chamber [79]. The highest OCV and power density values were achieved using 3D cubic electrodes due to the increasing metabolic activity of microorganisms owing to high electrode surface areas for biofilm formation. The maximum OCV and power density values of 718 mV and 9.55 mW/m^3 were recorded at the end of the operating time of 8 days, respectively. However, the power density decreased from 9.55 mW/m^3 to 8.82 mW/m^3 at the end of 12 days. As mentioned above, a decrease in power generation might be attributed to the effect of decreased electron formation due to the depletion of organic matter resulting in a decrease of microbial activity.

Moreover, similar trends were observed for the CE and CR values using electrode types of plate and 3D cubic. The CE and CR values were 12.9% and 11.7% for plate type electrode and 13.1% and 11.9% for 3D cubic electrodes, respectively. The increase in CE and CR values using 3D cubic electrodes could be explained that as the considerable amount of anode chamber was filled with the 3D cubic electrodes, electron transfer was significantly accelerated due to a decrease in the internal resistance. Consequently, in addition to the advantages mentioned above, this novel MDC could also facilitate MDC's real-scale operations considering the ease of operation of electrode materials, high energy production, in addition to comparable desalination and wastewater treatment efficiencies.

3.4. Geothermal water treatment

MDC was operated with plate and 3D cubic electrodes, treating real geothermal water at optimized conditions. Measured power density, OCV, effluent boron, and COD concentrations were presented in Fig. 5. As expected, the boron removal efficiency increased with 3D cubic electrodes. The highest boron removal efficiencies were found to be 44.3% ($C_{f,B}$: 5.836 mg/L) and 55.5% ($C_{f,B}$: 4.658 mg/L) for plate and 3D cubic electrodes, respectively. The initial EC value for the geothermal water was measured as 1770 μS/cm. Although the treated geothermal water's final EC value was not measured for 3D-MDC setup, it was recorded as 53.82 μS/cm for the 2D-MDC setup. Given that the boron removal efficiency has been enhanced with the 3D-MDC setup, the final EC value measured at the desalination chamber would be expected to be lower than the value acquired with the 2D-MDC setup. Observed boron removal efficiency for real geothermal water (55.5%) was lower than that for 5 mg/L boron synthetic solution (64.9%) for the 3D electrodes

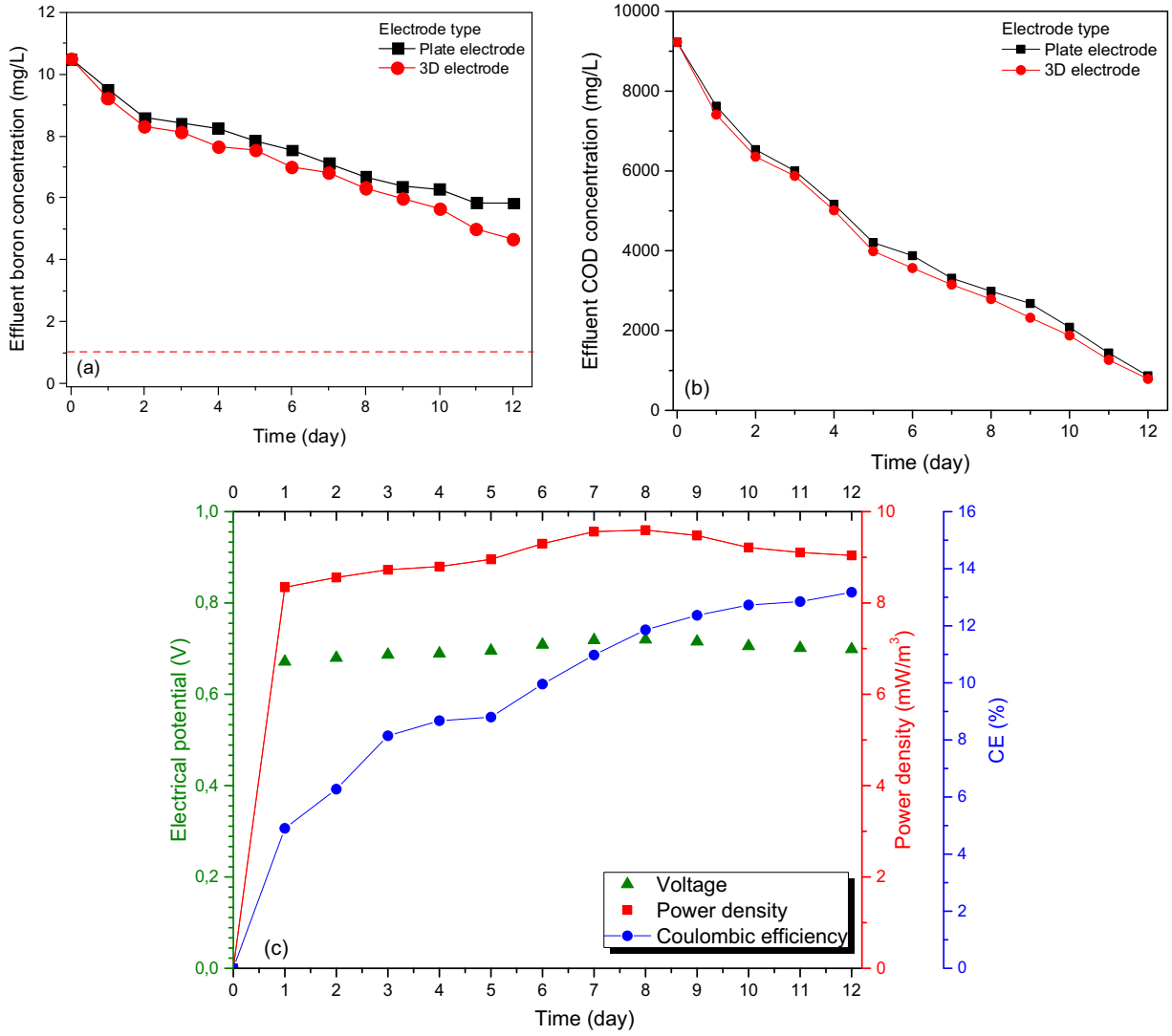

Fig. 5. Effect of electrode type on geothermal water treatment: boron removal (a), COD removal (b), voltage (c), power density (d).

under same experimental conditions. This was most probably due to the high boron content of the real geothermal water. Besides, real geothermal water contains other molecules such as anions, cations, and heavy metals. Competition between boron and other species in water might decrease the mass transfer ratio of boron from desalination chamber to anode chamber. Furthermore, the maximum COD removal efficiency was 91.5% ($C_{f,COD}$: 786 mg/L) for 3D cubic electrodes, while it was 90.6% ($C_{f,COD}$: 856 mg/L) for 2D electrodes. The maximum OCV of 699 mV and power density of 9.04 mW/m^3 were recorded at the end of the operating time of 12 days for 3D electrodes. The highest CE and CR values of 13.2% and 12.1% were achieved using 3D cubic electrodes. These results confirmed that the novel MDC with 3D cubic electrodes showed comparable boron removal, industrial wastewater efficiency, and energy production for treating real geothermal water.

3.5. Membrane fouling and biofilm formation

Biofilm formation occurs on the surface of AEM-anode side due to microbial colonization [80,81]. Biofilm formation on the surface of AEM, which is called as biofouling, widely occurs when the MDC system has been operated for a long time. AEM's structural integrity, stability, and functional groups on the surface is compromised due to the growth of biofilm, resulting in deposition of organic matter on AEM surface. This phenomenon causes the increase in internal resistance of the system, which adversely affects the performance of MDC process [82].

Fig. 6 demonstrated the SEM images of AEM and CEM surfaces. At the end 12 days, visible deformations and color change on AEM- anode side were observed. The color of the AEM was changed from light brown to black at the high activated sludge volumes, while this change was observed less for the low activated sludge volume. Furthermore, as presented in Fig. 6a, the AEM surface facing the anode chamber showed formation of biofilm at the surface of the membrane due to direct contact of the AEM to mixture of industrial wastewater and anaerobic activated sludge. On the other hand, AEM-desalination side demonstrated considerable crystalline salt accumulation (Fig. 6b). Similarly, the CEM on both sides showed crystalline salt aggregates (Fig. 6c and d). On the other hand, there was no biofilm formation on both CEM surfaces as they were isolated from microorganisms.

Furthermore, the EDX results identified salt content on the membrane surfaces (Table 1). The EDX results showed a considerable accumulation of chloride and boron on the AEM surfaces facing both desalination and anode chambers. Boron accumulation on the AEM surfaces were found to be 26.91% and 30.31% for surfaces facing the anode and desalination chambers, respectively. Boron and chloride accumulations on both sides of the AEM were mainly due to the transfer of anions from the desalination to anode chamber. On the other hand, carbon and sulfate contents of the AEM-anode side were not only measured lower than those of the unused AEM but they were also lower

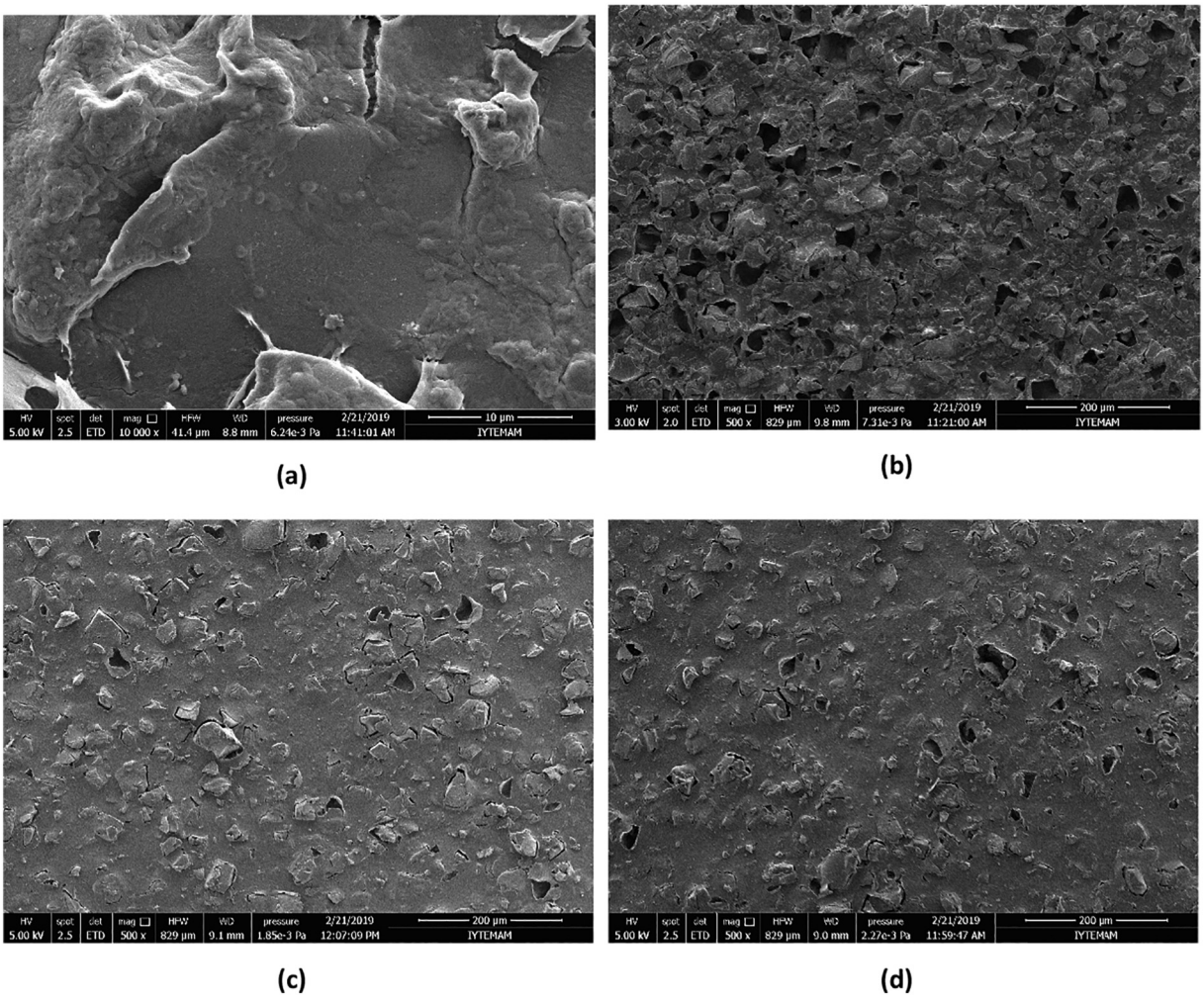

Fig. 6. SEM images of membranes after operation. AEM surface in anolyte solution (a), AEM surface in desalination solution (b), CEM surface in catholyte solution (c), CEM surface in solution (d).

Table 1
EDX results of the membranes before and after the experiment.

Material (Wt, %)	C	O	S	Na	F	Cl	B
AEM-Fresh	60.15	–	1.15	0.55	38.16	–	–
AEM (anode solution side)	50.50	2.75	0.15	–	10.67	0.25	30.31
AEM (desalination solution side)	56.01	3.12	0.38	–	13.20	0.38	26.91
CEM-Fresh	51.12	–	3.48	–	44.85	–	–
CEM (cathode solution side)	41.02	6.08	3.51	2.53	36.81	–	–
CEM (desalination solution side)	50.96	4.38	2.97	3.99	36.75	–	–

than those of the AEM-desalination side. This could be due to consumption of carbon and sulfate by microorganisms, which colonized and formed biofilm on membrane surface.

Oxygen deposition on CEM-cathode side was most probably due to the aerated catholyte solution, while the sodium deposition over the CEM-desalination side was due to desalination solution's pH being adjusted using NaOH solution. Other contents including, carbon, sulfate, and fluoride observed in the EDX results were ascribed to the inherent composition of the CEM polymer. Results showed that the membrane fouling mechanisms due to formation of biofilm and salt accumulation were important problems that prevented long-term stability of the system and needed to be further investigated. 36 day-long experiments with the 2D-MDC setup (S:WW ratio of 1:1, electrode surface area of 36 cm^2, catholyte solution of PBS buffer, and air flow rate of 2 L/min) revealed that boron removal rates have significantly decreased in consecutive cycles of 12 days for initial boron concentrations of 5, 10 and 20 mg/L [51].

Coating of AEM with nanomaterials may considerably prevent biofilm formation and improve its structural integrity and stability, which may in turn extend its service time and reusability, and enhance efficiency of the MDC process [83]. Moreover, the AEM fouling problem can be solved with developing effective polymers that may perform steadily with a wide range of temperature and pH values. For instance, the AEM crossed linked with wood-lignin may be a promising option since lignin has a number of desirable features, one of which is its stability [54]. Scaling with accumulation of anions and cations on AEM surface is another severe problem when real wastewater and seawater are treated. Several studies have been conducted to prevent or eliminate membrane fouling [84]. Researchers focused on synthesis of membrane materials integrated with antifouling features to prevent membrane fouling [85]. However, synthesis of antifouling membranes may be impractical to eliminate various types of fouling at once. Therefore, more investigation is needed to enhance the efficiency of existing modified AEMs and elucidate the main mechanism of fouling through understanding characteristics of fouling types.

3.6. Control experiment

In a previous study, a negative control experiment using the 2D-MDC set up was done using 5 mg/L initial boron concentration in the absence of microbial activity. All other operating parameters were kept the same. As a result, only 26.2% of boron was removed from the desalination chamber, pointing to a significant impairment in diffusion rate due to lack of electrochemical gradient [51]. Moreover, another control experiment was done under optimum operating conditions (initial boron concentration of 5 mg/L, S:WW ratio of 1:1, electrode surface area of 36 cm^2, catholyte solution of PBS buffer, and air flow rate of 2 L/min) at open circuit for both 2D-MDC and 3D-MDC. The removed boron content was found to be 2.52 and 2.80 mg/L for 2D-MDC and 3D MDC at open circuit mode, respectively. The amount of removed boron was lower than that achieved with the closed circuit mode for both 2D-MDC (3.07 mg/L) and 3D-MDC (3.244 mg/L). These results showed that the boron diffusion increased with the increase in the electrochemical gradient, improving the removal efficiency.

4. Conclusion

Desalination of geothermal wastewater is crucial for its reuse in agricultural irrigation in water scarce regions. Simultaneous boron and organic matter removal with energy production were effectively achieved using novel MDC with 3D cubic electrodes. It was found that the anolyte solution temperature, S:WW ratio, and electrode type significantly affected performance of MDC. According to results, novel MDC achieved the maximum boron and organic matter removal efficiencies of 64.9% and 90.7%, respectively, with the highest power density of 9.55 mW/m^3 for 5 mg/L of boron containing synthetic solution. The highest boron and organic matter removal efficiencies were 55.5% and 91.5% with the maximum power density of 9.04 mW/m^3 for real geothermal water. Achieved results were comparable with conventional MDC runs, however it should be noted that if the designed electrode cell was filled with 3D cubic electrodes the removal efficiencies and energy production performance were expected to improve. SEM and EDX results presented significant biofilm formation on AEM facing the anode chamber and salt deposition on the both AEM and CEM at the end of the operation and showed that biofilm formation and salt deposition may adversely affect the performance of MDC, particularly in the operation with higher activates sludge: wastewater ratio. Therefore, there is need for further investigation on membrane scaling by biofilm formation and salt decomposition to enhance the performance of MDC process. Consequently, our results showed that the novel MDC was a promising process for boron and organic matter removal with energy production during industrial wastewater and geothermal water treatment.

CRediT authorship contribution statement

Aysegul Yagmur Goren: Writing-Original draft preparation, Investigation, Validation; **Hatice Eser Okten**: Supervision, Reviewing and Editing, Conceptualization, Resources.

Declaration of competing interest

The authors declare that they have no known competing financial interests or personal relationships that could have appeared to influence the work reported in this paper.

Acknowledgement

Authors would like to thank to Environmental Development, Application and Research Center at Izmir Institute of Technology for boron analyses. Authors would like to thank to Center for Materials Research for SEM analyses. Part of this study was funded by IZTECH Scientific Research Projects Coordinatorship, grant number 2017IYTE62.

Appendix A. Supplementary data

Supplementary data to this article can be found online at https://doi.org/10.1016/j.desal.2021.115267.

References

[1] A. Baba, H. Armansson, Environmental impact of the utilization of geothermal areas, Energy Sources Part B 1 (2006) 267–278.
[2] N. Aksoy, C. Simsek, O. Gunduz, Groundwater contamination mechanism in a geothermal field: a case study of Balcova, Turkey, J. Contam. Hydrol. 103 (2009) 13–28.
[3] F.S. Tut Haklidir, R. Sengün, Hydrogeochemical similarities and diferences between high temperature geothermal systems with similar geologic settings in the Büyük Menderes and Gediz grabens of Turkey, Geothermics 83 (2020), 101717.
[4] E. Villalba, C. Tanjal, G. Borzi, G. Páez, E. Carol, Geogenic arsenic contamination of wet-meadows associated with a geothermal system in an arid region and its relevance for drinking water, Sci. Total Environ. 720 (2020) (2020), 137571.
[5] D. Kartikaningsih, Y.J. Shih, Y.H. Huang, Boron removal from boric acid wastewater by electrocoagulation using aluminum as sacrificial anode, Sustain. Environ. Res. 26 (2016) 150–155.
[6] A.E. Yilmaz, R. Boncukoglu, M.M. Kocakerim, M.T. Yilmaz, C. Paluluoglu, Boron removal from geothermal waters by electrocoagulation, J. Hazard. Mater. 153 (2008) 146–151.
[7] S. Barth, Utilization of boron as a critical parameter in water quality for thermal and mineral water resources in SW german and N Switzerland, Environ. Geol. 40 (2000) 1–2.
[8] N. Kabay, M. Bryjak, Boron Separation Processes, in: Elsevier, Amsterdam, 2015, pp. 219–235.
[9] M. Bryjak, J. Wolska, N. Kabay, Removal of boron from seawater by adsorption membrane hybrid process: implementations and challenges, Desalination 223 (2008) 57–62.
[10] F.H. Nielsen, The nutritional importance and pharmacological potential of boron for higher animals and human, in: H.E. Goldbach, P.H. Brown, B. Rerkasem, M. Thellier, M.A. Wimmer, R.W. Bell (Eds.), Boron in Plant and Animal Nutrition, Springer, Boston, MA, 2002, pp. 37–49.
[11] L. Melnyk, V. Goncharuk, I. Butnyk, E. Tsapiuk, Boron removal from natural and wastewaters using combined sorption/membrane process, Desalination 185 (2005) 147–157.
[12] D. Hou, J. Wang, X. Sun, Z. Luan, C. Zhao, X. Ren, Boron removal from aqueous solution by direct contact membrane distillation, J. Hazard. Mater. 177 (2010) 613–619.
[13] World Health Organization (WHO), in: Environmental Health criteria 204: Boron, 1998.
[14] European Communities (EC), Council Directive 98/83/EC of 3 November 1998 on the quality of water intended for human consumption, Off. J. Eur. Communities 330 (1998) 32–54.
[15] Official Journal, Regulation on Water Intended for Human Consumption, 28580, 07 March 2013, Ankara (in Turkish), 2013.
[16] N. Hilal, G.J. Kim, C. Somerfield, Boron removal from saline water: a comprehensive review, Desalination 273 (2011) 23–35.
[17] F. García-Sánchez, S. Simón-Grao, J.J. Martínez-Nicolás, M. Alfosea-Simón, C. Liu, C. Chatzissavvidis, J.G. Pérez-Pérez, J.M. Cámara-Zapata, Multiple stresses occurring with boron toxicity and deficiency in plants, J. Hazard. Mater. 397 (2020), 122713.
[18] M. Chen, O. Dollar, K. Shafer-Peltier, S. Randtke, S. Waseem, E. Peltier, Boron removal by electrocoagulation: removal mechanism, adsorption models and factors influencing removal, Water Res. 170 (2020), 115362.
[19] A. Hussain, R. Sharma, J. Minier-Matar, Z. Hirani, S. Adham, Application of emerging ion exchange resin for boron removal from saline groundwater, J. Water Process. Eng. 32 (2019), 100906.
[20] I. Skoczko, Boron removal from the water with chemical precipitation methods, Desalin. Water Treat. 186 (2020) 430–436.
[21] S.H. Ban, S.J. Im, J. Cho, A. Jang, Comparative performance of FO-RO hybrid and two-pass SWRO desalination processes: boron removal, Desalination 471 (2019), 114114.
[22] S. Kayaci, S.B. Tantekin-Ersolmaz, M.G. Ahunbay, W.B. Krantz, Technical and economic feasibility of the concurrent desalination and boron removal (CDBR) process, Desalination 486 (2020), 114474.
[23] T. Jafary, A. Al-Mamun, H. Alhimali, M.S. Baawain, S. Rahman, W.A. Tarpeh, B. R. Dhar, B.H. Kim, Novel two-chamber tubular microbial desalination cell for bioelectricity production, wastewater treatment and desalination with a focus on self-generated pH control, Desalination 481 (2020), 114358.
[24] C.Y. Ma, C.H. Hou, Enhancing the water desalination and electricity generation of a microbial desalination cell with a three-dimensional macroporous carbon nanotube-chitosan sponge anode, Sci. Total Environ. 675 (2019) 41–50.
[25] Y. Kim, B.E. Logan, Microbial desalination cell for energy production and desalination, Desalination 308 (2013) 122–130.
[26] Q. Ping, I.M. Abu-Reesh, Z. He, Boron removal from saline water by a microbial desalination cell integrated with Donnan dialysis, Desalination 376 (2015) 55–61.
[27] Q. Ping, I.M. Abu-Reesh, Z. He, Mathematical modeling based evaluation and simulation of boron removal in bioelectrochemical systems, Sci. Total Environ. 569–570 (2016) 1380–1389.

[28] K. Zuo, M. Chen, F. Liu, K. Xiao, J. Zuo, X. Cao, X. Zhang, P. Liang, X. Huang, Coupling microfiltration membrane with biocathode microbial desalination cell enhances advanced purification and long-term stability for treatment of domestic wastewater, J. Membr. Sci. 547 (2018) 34–42.
[29] H. Wang, G. Wang, Y. Ling, F. Qian, Y. Song, X. Lu, S. Chen, Y. Tong, Y. Li, High power density microbial fuel cell with flexible 3D graphene–nickel foam as anode, Nanoscale 5 (2013) 10283–10290.
[30] D. Pant, G. Van Bogaert, L. Diels, K. Vanbroekhoven, A review of the substrates used in microbial fuel cells (MFCs) for sustainable energy production, Bioresour. Technol. 101 (2010) 1533–1543.
[31] X. Zhang, X. Li, X. Zhao, Y. Li, Factors affecting the efficiency of a bioelectrochemical systems: a review, RSC Adv. 9 (2019) 19748.
[32] S. Li, C. Cheng, A. Thomas, Carbon-based microbial-fuel-cell electrodes: from conductive supports to active catalysts, Adv. Mater. 29 (2017) 8.
[33] P.Y. You, S.K. Kamarudin, Recent progress of carbonaceous materials in fuel cell applications: an overview, Chem. Eng. J. 309 (2017) 489–502.
[34] M.H. Do, H.H. Ngo, W.S. Guo, Y. Liu, S.W. Chang, D.D. Nguyen, L.D. Nghiem, B. J. Ni, Challenges in the application of microbial fuel cells to wastewater treatment and energy production: a mini review, Sci. Total Environ. 639 (2018) 910–920.
[35] D.Z. Sun, Y.Y. Yu, R.R. Xie, C.L. Zhang, Y. Yang, D.D. Zhai, G. Yang, L. Liu, Y. C. Yong, In-situ growth of graphene/polyaniline for synergistic improvement of extracellular electron transfer in bioelectrochemical systems, Biotechnol. Bioeng. 87 (2017) 195–202.
[36] B. Wang, Z. Wang, Y. Jiang, G. Tan, N. Xu, Y. Xu, Enhanced power generation and wastewater treatment in sustainable biochar electrodes based bioelectrochemical system, Bioresource Technol. 241 (2017) 841–848.
[37] H.R. Yuan, L.F. Deng, X. Qian, L.F. Wang, D.N. Li, Y. Chen, Y. Yuan, Significant enhancement of electron transfer from shewanella oneidensis using a porous N-doped carbon cloth in a bioelectrochemical system, Sci. Total Environ. 665 (2019) 882–889.
[38] D.J. Ahirrao, S. Tambat, A.B. Pandit, N. Jha, Sweet-lime-peels-derived activated-carbon-based electrode for highly efficient supercapacitor and flow-through water desalination, Energy Environ. Sci. 4 (2019) 2610–2625.
[39] M. Ramirez-Moreno, A. Esteve-Núñez, J.M. Ortiz, Desalination of brackish water using a microbial desalination cell: analysis of the electrochemical behavior, Electrochim. Acta 388 (2021), 138570.
[40] R. Liaquat, T. Mehmood, A.H. Khoja, N. Iqbal, H. Ejaz, S. Mumtaz, Investigating the potential of locally sourced wastewater as a feedstock of microbial desalination cell (MDC) for bioenergy production, Bioprocess Biosyst. Eng. 44 (2021) 173–184.
[41] S. Rahman, A. Al-Mamun, T. Jafary, H. Alhimali, M.S. Baawain, Effect of internal and external resistances on desalination in microbial desalination cell, Water Sci. Technol. 83 (2021) 2389–2403.
[42] Y. Kim, B.E. Logan, Series assembly of microbial desalination cells containing stacked electrodialysis cells for partial or complete seawater desalination, Environ. Sci. Technol. 45 (2011) 5840–5845.
[43] Z. Ge, C.G. Dosoretz, Z. He, Effects of number of cell pairs on the performance of microbial desalination cells, Desalination 341 (2014) 101–106.
[44] M. Hemalatha, S.K. Butti, G. Velvizhi, M.S. Venkata, Microbial mediated desalination for ground water softening with simultaneous power generation, Bioresour. Technol. 242 (2017) 28–35.
[45] A. Al-Mamun, W. Ahmad, M.S. Baawain, M. Khadem, B.R. Dhar, A review of microbial desalination cell technology: configurations, optimization and applications, J. Clean. Prod. 183 (2018) 458–480.
[46] A. Ebrahimi, G.D. Najafpour, D.Y. Kebria, Performance of microbial desalination cell for salt removal and energy generation using different catholyte solutions, Desalination 432 (2018) 1–9.
[47] M. Malakootian, H. Mahdizadeh, A. Nasiri, F. Mirzaienia, M. Hajhoseini, N. Amirmahani, Investigation of the efficiency of microbial desalination cell in removal of arsenic from aqueous solutions, Desalination 438 (2018) 19–23.
[48] APHA (American Public Health Association), Standard Methods for the Examination of Water and Wastewater, Washington, DC, 2005.
[49] B. Ozbey-Unal, D.Y. Imer, B. Keskinler, I. Koyuncu, Boron removal from geothermal water by air gap membrane distillation, Desalination 433 (2018) 141–150.
[50] A. Baba, H. Sözbilir, Source of arsenic based on geological and hydrogeochemical properties of geothermal systems in Western Turkey, Chem. Geol. 334 (2012) 364–377.
[51] A.Y. Goren, H.E. Okten, Energy production from treatment of industrial wastewater and boron removal in aqueous solutions using microbial desalination cell, Chemosphere 285 (2021), 131370.
[52] APHA, American Public Health Association Manual, Standard Methods for the Examination of Water and Wastewater, Parts 4000-6000, 2017.
[53] P. Noori, N.G. Darzi, Enhanced power generation in annular single-chamber microbial fuel cell via optimization of electrode spacing using chocolate industry wastewater, Biotechnol. Appl. Biochem. 63 (2016) 427–434.
[54] M. Tawalbeh, A. Al-Othman, K. Singh, I. Douba, D. Kabakebji, M. Alkasrawi, Microbial desalination cells for water purification and power generation: a critical review, Energy 209 (2020), 118493.
[55] A. Gholizadeh, A.A. Ebrahimi, M.H. Salmani, M.H. Ehrampoush, Ozone-cathode microbial desalination cell; an innovative option to bioelectricity generation and water desalination, Chemosphere 188 (2017) 470–477.
[56] P. Tamta, N. Rani, A.K. Yadav, Enhanced wastewater treatment and electricity generation using stacked constructed wetlandemicrobial fuel cells, Environ. Chem. Lett. May. 218 (2020) 871–879.
[57] H.H. Salman, Z.Z. Ismail, Desalination of actual wetland saline water associated with biotreatment of real sewage and bioenergy production in microbial desalination cell, Sep. Purif. Technol. 250 (2020), 117110.
[58] F. Meng, Q. Zhao, Z. Zheng, L. Wei, K. Wang, J. Jiang, J. Ding, X. Na, Simultaneous sludge degradation, desalination and bioelectricity generation in two-phase microbial desalination cells, Chem. Eng. J. 361 (2019) 180–188.
[59] M. Tawalbeh, A.S. Rajangam, T. Salameh, A. Al-Othman, M. Alkasrawi, Characterization of paper mill sludge as a renewable feedstock for sustainable hydrogen and biofuels production, Int. J. Hydrog. Energy 46 (2021) 4761–4775.
[60] T.S. Utami, R. Arbianti, B.N. Manaf, Sea water desalination using Debaryomyces hansenii with microbial desalination cell technology, Int. J. Technol. 6 (2015) 1094–1100.
[61] M.A. Rodrigo, P. Canizares, J. Lobato, R. Pazz, C. Saez, J.J. Linares, Production of electricity from the treatment of urban waste using a microbial fuel cell, J. Power Sources 19 (2007) 198–204.
[62] A. Larrosa-Guerrero, K. Scott, I.M. Head, F. Mateo, A. Ginesta, C. Godinez, Effect of temperature on the performance of microbial fuel cells, Fuel 89 (2010) 3985–3994.
[63] O. Tkach, T. Sangeetha, S. Maria, A. Wang, Performance of low temperature microbial fuel cells (MFCs) catalyzed by mixed bacterial consortia, J. Environ. Sci. 52 (2017) 284–292.
[64] G.S. Jadhav, M.M. Ghangrekar, Performance of microbial fuel cell subjected to variation in pH, temperature, external load and substrate concentration, Bioresour. Technol. 100 (2009) 717–723.
[65] L. Wei, H. Han, J. Shen, Effects of temperature and ferrous sulfate concentrations on the performance of microbial fuel cell, Int. J. Hydrog. Energy 38 (2013) 11110–11116.
[66] Y. Song, J. An, K.J. Chae, Effect of temperature variation on the performance of microbial fuel cells, Energ. Technol. 5 (2017) 2163–2167.
[67] M. Malakootian, F. Mirzaienia, M. Malakootian, Removal efficiency of Cu2 and Zn2 from industrial wastewater by using microbial desalination cell, J. Water Chem. Techno. 41 (2019) 334–339.
[68] M. Ragab, A. Elawwad, H. Abdel-Halim, Evaluating the performance of microbial desalination cells subjected to different operating temperatures, Desalination 462 (2019) 56–66.
[69] L. Leven, A.R.B. Eriksson, A. Schnürer, Effect of process temperature on bacterial and archaeal communities in two methanogenic bioreactors treating organic household waste, FEMS Microbiol. Ecol. 59 (2007) 683–693.
[70] E. Sanchez, R. Borja, P. Weiland, L. Travieso, A. Martin, Effect of temperature and pH on the kinetics of methane production, organic nitrogen and phosphorus removal in the batch anaerobic digestion process of cattle manure, Bioprocess Eng. 22 (2000) 247–252.
[71] J. Zabranska, J. Stepova, R. Wachtl, P. Jenicek, M. Dohanyos, The activity of anaerobic biomass in thermophilic and mesophilic digesters at different loading rates, Water Sci. Technol. 42 (2000) 49–56.
[72] K.S. Jacobson, D.M. Drew, Z. He, Efficient salt removal in a continuously operated upflow microbial desalination cell with an air cathode, Bioresour. Technol. 102 (2011) 376–380.
[73] F. Mirzaienia, A. Asadipour, A.J. Jafari, M. Malakootian, Removal efficiency of nickel and lead from industrial wastewater using microbial desalination cell, Appl Water Sci 7 (2017) 3617–3624.
[74] C.P.L. Grady, G.T. Daigger, H.C. Lim, Biological Wastewater Treatment, Marcel Dekker, New York, 1999.
[75] J. Larminie, A. Dicks, Fuel Cell Systems Explained, Second edition, Wiley, New York, 2003.
[76] A.J. Bard, L.R. Faulkner, Electrochemical Methods, Fundamentals and Applications, Wiley, New York, 2001.
[77] C.H. Hou, N.L. Liu, H.L. Hsu, W. Den, Development ofmulti-walled carbon nanotube/poly(vinyl alcohol) composite as electrode for capacitive deionization, Sep. Purif. Technol. 130 (2014) 7–14.
[78] H. Yuan, G. Dong, D. Li, L. Deng, P. Cheng, Y. Chen, Steamed cake-derived 3D carbon foam with surface anchored carbon nanoparticles as freestanding anodes for high-performance microbial fuel cells, Sci. Total Environ. 636 (2018) 1081–1088.
[79] S. Venkata-Mohan, S. Srikanth, P. Chiranjeevi, S. Arora, R. Chandra, Algal biocathode for in situ terminal electron acceptor (TEA) production: synergetic association of bacteria-microalgae metabolism for the functioning of biofuel cell, Bioresour. Technol. 166 (2014) 566–574.
[80] H. Luo, P. Xu, T.M. Roane, P.E. Jenkins, Z. Ren, Microbial desalination cells for improved performance in wastewater treatment, electricity production, and desalination, Bioresour. Technol. 105 (2012) 60–66.
[81] X. Zhu, M.D. Yates, M.C. Hatzell, H. Ananda Rao, P.E. Saikaly, B.E. Logan, Microbial community composition is unaffected by anode potential, Environ. Sci. Technol. 48 (2014) 1352–1358.
[82] H. Luo, P. Xu, Z. Ren, Long-term performance and characterization of microbial desalination cells in treating domestic wastewater, Bioresour. Technol. 120 (2012) 187–193.
[83] L. Guang, D.A. Koomson, H. Jingyu, D. Ewusi-Mensah, N. Miwornunyuie, Performance of exoelectrogenic bacteria used in microbial desalination cell technology, Int. J. Environ. Res. Public Health 17 (2020) 1121.
[84] M.N.I. Salehmin, S.S. Lim, I. Satar, W.R.W. Daud, Pushing microbial desalination cells towards field application: prevailing challenges, potential mitigation strategies, and future prospects, Sci. Total Environ. 759 (2021), 143485.
[85] M. Vaselbehagh, H. Karkhanechi, S. Mulyati, R. Takagi, H. Matsuyama, Improved antifouling of anion-exchange membrane by polydopamine coating in electrodialysis process, Desalination 332 (2014) 126–133.